



CrossMark
click for updates

Research

Cite this article: Groen D, Borgdorff J, Bona-Casas C, Hetherington J, Nash RW, Zasada SJ, Saverchenko I, Mamonski M, Kurowski K, Bernabeu MO, Hoekstra AG, Coveney PV. 2013 Flexible composition and execution of high performance, high fidelity multiscale biomedical simulations. *Interface Focus* 3: 20120087.

<http://dx.doi.org/10.1098/rsfs.2012.0087>

One contribution of 25 to a Theme Issue 'The virtual physiological human: integrative approaches to computational biomedicine'.

Subject Areas:

bioinformatics, computational biology

Keywords:

multiscale modelling, blood flow, high performance computing, in-stent restenosis, cerebrovascular bloodflow, distributed computing

Authors for correspondence:

D. Groen

e-mail: d.groen@ucl.ac.uk

P. V. Coveney

e-mail: p.v.coveney@ucl.ac.uk

Electronic supplementary material is available at <http://dx.doi.org/10.1098/rsfs.2012.0087> or via <http://rsfs.royalsocietypublishing.org>.

Flexible composition and execution of high performance, high fidelity multiscale biomedical simulations

D. Groen¹, J. Borgdorff², C. Bona-Casas², J. Hetherington¹, R. W. Nash¹, S. J. Zasada¹, I. Saverchenko³, M. Mamonski⁴, K. Kurowski⁴, M. O. Bernabeu¹, A. G. Hoekstra² and P. V. Coveney¹

¹Centre for Computational Science, University College London, UK

²Section Computational Science, University of Amsterdam, The Netherlands

³Leibniz-Rechenzentrum, Garching, Germany

⁴Poznan Supercomputing and Networking Center, Poznan, Poland

Multiscale simulations are essential in the biomedical domain to accurately model human physiology. We present a modular approach for designing, constructing and executing multiscale simulations on a wide range of resources, from laptops to petascale supercomputers, including combinations of these. Our work features two multiscale applications, in-stent restenosis and cerebrovascular bloodflow, which combine multiple existing single-scale applications to create a multiscale simulation. These applications can be efficiently coupled, deployed and executed on computers up to the largest (peta) scale, incurring a coupling overhead of 1–10% of the total execution time.

1. Introduction

Models of biomedical systems are inherently complex; properties on small time and length scales, such as the molecular or genome level, can make a substantial difference to the behaviour observed on much larger scales, such as the organ, full-body and even the population level; and vice versa [1,2]. We therefore need to apply multiscale approaches when modelling many biomedical situations. Examples of multiscale biomedical challenges include predicting the impact of a surgical procedure [3], investigating the effects of pathologies (e.g. arterial malformations and fistulas [4]) or assessing the effects of a targeted drug on a given patient [5]. In all these cases, we need to examine processes that not only occur across several time and/or length scales, but that also rely on different underlying physical and/or biological mechanisms. As a result, modelling these processes may require substantially different algorithms and varying levels of computational effort.

Historically, these problems have often been modelled using single-scale approaches, focusing exclusively on those aspects of the problem which are deemed most relevant. However, applying a single-scale model is frequently insufficient to fully understand the problem at hand, as additional processes occurring on different scales must be incorporated to obtain sufficient accuracy. It is this need for understanding the composite problem, rather than its individual subcomponents alone, that has driven many research groups to explore multiscale modelling [6–9].

In a multiscale model, the overall system is approximated by coupling two or more single-scale *submodels*. Establishing and performing the data exchange between these submodels is an important aspect of enabling multiscale modelling. It is often addressed by using coupling tools, such as the Multiscale Library and Coupling Environment (MUSCLE) [10,11], the Multilevel Communicating Interface [12] and GridSpace [13]. Groen *et al.* [14] provide a review of coupling tools and the computational challenges they address.

Another important aspect is adopting a data standard which submodels can adopt to exchange meaningful information. Several markup languages, such as SBML [15] and CellML [16], resolve this problem by providing a description language for the storage and exchange of model data and submodel definitions. CellML specifically allows for submodel exchange between ODE and PDE solvers, whereas SBML is aimed towards biochemical pathway and reaction ODE submodels. Both SBML and CellML, being languages for the description of submodels and system data, have serious limitations in that they require additional tools to perform tasks that are not directly related to ensuring data interoperability. These include transferring data between submodels, deploying submodels on appropriate resources and orchestrating the interplay of submodels in a multiscale simulation. Additionally, they only provide very limited features to describe submodels that do not rely on ODE-based methods, such as finite-element/volume methods, spectral methods, lattice-Boltzmann, molecular dynamics and particle-based methods, which are of increasing importance in the biomedical domain.

Here, we present a comprehensive approach to enable multiscale biomedical modelling from problem definition through the bridging of length and time scales, to the deployment and execution of these models as multiscale simulations. Our approach, which has been developed within the MAPPER project (<http://www.mapper-project.eu/>), relies on coupling existing submodels and supports the use of resources ranging from a local laptop to large international supercomputing infrastructures, and distributed combinations of these. We present our approach for describing multiscale biomedical models in §2 and for constructing and executing multiscale simulations on large computing infrastructures in §3. We describe our approach for biomedical applications in §4. We have applied our approach to two biomedical multiscale applications, in-stent restenosis (ISR) and hierarchical cerebrovascular blood flow (BF), which we present in §§5 and 6, respectively. We conclude with a brief discussion.

2. Multiscale biomedical modelling

Multiscale modelling gives rise to a number of challenges which extend beyond the translation of model and system data. Most importantly, we seek to allow application developers, such as computational biologists and biomedics, to couple multiscale models for large problems, supporting any type of coupling, using any type of submodel they wish to include, and executing this using any type of computational resource, from laptop to petascale. As we cannot expect computational biologists to have expertise in all the technical details of multiscale computing, we also aim to present a uniform and easy-to-use interface which retains the power of the underlying technology. This also enables users with less technical expertise to execute previously constructed multiscale simulations.

Multiscale systems are, in general, characterized by the interaction of phenomena on different scales, but the details vary for different scientific domains. To preserve the generality of our approach, we adopt the multiscale modelling and simulation framework (MMSF) to reason about multiscale models in a domain-independent context and to create *recipes* for constructing multiscale simulations independent of the underlying implementations or computer architectures. This MMSF is based on earlier work on coupled cellular automata

and agent-based systems [17,18] and has been applied to several computational problems in biomedicine [3,19,20]. Within the MMSF, the interactions between single-scale submodels are confined to well-defined couplings. The submodels can therefore be studied as independent models with dependent incoming and outgoing links. The graph of all submodels and couplings, the coupling topology, can either be cyclic or acyclic [21]. In a cyclic coupling topology, the submodels will exchange information in an iterative loop, whereas in an acyclic topology the submodels are activated one after another, resulting in a directional data flow which makes them well-suited for workflow managers. Two parts of the MMSF are particularly useful for our purposes, namely the *Scale Separation Map* [17] and the *multiscale modelling language* (MML) [11,22]. The Scale Separation Map is a graphical representation which provides direct insights into the coupling characteristics of the multiscale application. MML provides a formalization of the coupling between the submodels, independent of the underlying implementation. In addition, it simplifies the issues associated with orchestrating submodels by capturing the orchestration mechanisms in a simple model which consists of only four distinct operators. MML definitions can be stored for later use using an XML-based file format (xMML) or represented visually using graphical MML (gMML) [11].

The generic MML definitions allow us to identify commonalities between multiscale applications in different scientific domains. Additionally, the stored xMML can be used as input for a range of supporting tools that facilitate multiscale simulations (e.g. tools that automate the deployment or the submodel coupling of these simulations, as discussed in §3).

3. From multiscale model to production simulation

We have developed a range of tools that allow us to create, deploy and run multiscale simulations based on the xMML specification of a multiscale model. Two of the main challenges in realizing successful multiscale simulations are to establish a fast and flexible coupling between submodels and to deploy and execute the implementations of these submodels efficiently on computer resources of any size. In this section, we review these challenges and present our solutions to them.

3.1. Coupling submodels

Effective and efficient coupling between submodels encompasses three major aspects. First, we must translate our MML definitions to technical recipes for the multiscale simulation execution. Second, we need to initiate and orchestrate the execution of the submodels in an automated way, in accordance with the MML specification. Third, we need to efficiently exchange model and system information between the submodels.

The MUSCLE [10,11] provides a solution to the first two aspects. It uses MML in conjunction with a definition of the requested resources to bootstrap and start the different submodels and to establish a connection for data exchange between the submodels. It also implements the coupling definitions defined in the MMSF to orchestrate the submodels. The submodels can be coupled either locally (on a workstation, for example),

via a local network, or via a wide area network using the MUSCLE Transport Overlay (MTO) [23]. Running submodels in different locations and coupling them over a wide area network is especially important when submodels have very different computational requirements, for example when one submodel requires a local machine with a set of Python libraries, and another submodel requires a large supercomputer. However, messages exchanged across a wide area network do take longer to arrive. Among other things, MTO provides the means to exchange data between large supercomputers while adhering to the local security policies and access restrictions.

The exchanges between submodels overlap with computations in many cases (see §6 for an example), allowing for an efficient execution of the overall simulation. However, when the exchanges are particularly frequent or the exchanged data particularly large, inefficiencies in the data exchange can severely slow down the multiscale simulation as a whole. We use the MPWide communication library [24], previously used to run cosmological simulations distributed across supercomputers [25], to optimize our wide area communications for performance. We already use MPWide directly within the cerebrovascular bloodflow simulation and are currently incorporating it in MUSCLE to optimize the performance of the MTO.

3.2. Deploying and executing submodels on production resources

When large multiscale models are deployed and executed as simulations on production compute resources, a few major practical challenges arise. Production resources are often shared by many users, and are difficult to use even partially at appropriate times. This in turn makes it difficult to ensure that the submodels are invoked at the right times, and in cases where they are distributed on different machines, to ensure that the multiscale simulation retains an acceptable time to completion. We use the QosCosGrid environment (QCG) [26] to run submodels at a predetermined time on large computing resources. QCG enables us, if installed on the target resource, to reserve these resources in advance for a given period of time to allow our submodels to be executed there. This is valuable in applications that require cyclic coupling, as we then require multiple submodels to be executed either concurrently or in alternating fashion. Additionally, with QCG we can explicitly specify the sequence of resources to be reserved, allowing us to repeat multiple simulations in a consistent manner using the same resource sequence each time. A second component that aids in the execution of submodels is the application hosting environment (AHE) [27]. AHE simplifies user access to production resources by streamlining the authentication methods and by centralizing the installation and maintenance tasks of application codes. The end users of AHE only need to work with one uniform client interface to access and run their applications on a wide range of production resources.

4. Using MAPPER for biomedical problems

We apply the MAPPER approach to a number of applications. We present two of these applications here (ISR and cerebrovascular BF), but we have also used MAPPER to define, deploy and execute multiscale simulations of clay-

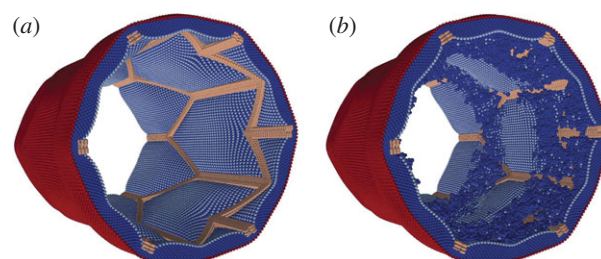


Figure 1. Images of a stented artery as modelled using ISR3D, before restenosis occurs on (a) and after 12.5 days of muscle cell proliferation on (b).

polymer nanocomposite materials [28], river beds and canals [29], and several problems in nuclear fusion.

MAPPER provides formalisms, tools and services which aid in the description of multiscale models, as well as the construction, deployment and execution of multiscale simulations on production infrastructures. It is intended as a general-purpose solution, and as such tackles challenges in multiscale simulation that exist across scientific disciplines. There are a number of challenges which are outside the scope of our approach, because they may require different solutions for different scientific disciplines. These include choosing appropriate submodels for a multiscale simulation and defining, on the application level, what information should be exchanged between submodels at which times to provide a scientifically accurate and stable multiscale simulation. However, MMSF does simplify the latter task by providing a limited number of orchestration mechanisms. The formalisms, tools and services presented here are independent components, allowing users to adopt those parts of our approach which specifically meet their requirements in multiscale modelling. This modular approach makes it easier for users to exploit the functionalities of individual components and helps to retain a lightweight simulation environment.

5. Modelling in-stent restenosis

Coronary heart disease (CHD) is one of the most common causes of death and is responsible for about 7.3 million deaths per year worldwide [30]. CHD is typically expressed as atherosclerosis, which corresponds with a thickening and hardening of blood vessels caused by build-up of atheromatous plaque; when this significantly narrows the vessel, it is called a stenosis. A common intervention for stenosis is stent-assisted balloon angioplasty where a balloon, attached to a stent, is inserted in the blood vessel and inflated at the stenosed location, consequently deploying the stent. The stent acts as a scaffold for the blood vessel, compressing the plaque and holding the lumen open. Occasionally, however, this intervention is followed by ISR, an excessive regrowth of tissue due to the injury caused by the stent deployment [31,32]. Although there are a number of different hypotheses [33], the pathophysiological mechanisms and risk factors of ISR are not yet fully clear.

By modelling ISR with a three-dimensional model (ISR3D), it is possible to test mechanisms and risk factors that are likely to be the main contributors to ISR. After evaluating the processes involved in ISR [19], ISR3D applies the hypothesis that smooth muscle cell (SMC) proliferation drives the restenosis, and that this is affected most heavily by wall shear stress of the BF, which regulates endothelium

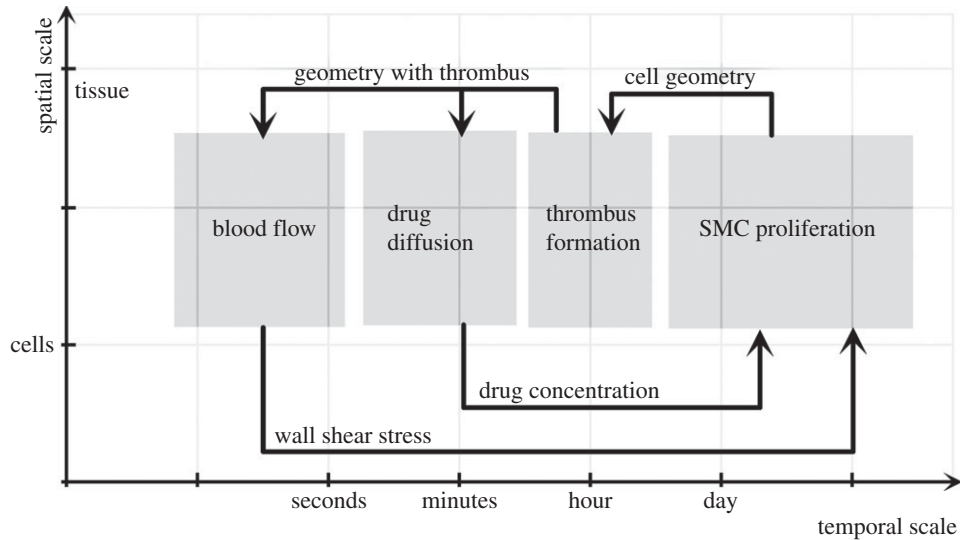


Figure 2. Scale Separation Map of the ISR3D multiscale simulation, originally presented in [11].

recovery, and by growth inhibiting drugs diffused by a drug-eluting stent. Using the model, we can evaluate the effect of different drug intensities, physical stent designs, vascular geometries and endothelium recovery rates. ISR3D is derived from the two-dimensional ISR2D [3,20] code. Compared with ISR2D, it provides additional accuracy, incorporating a full stent design, realistic cell growth and a three-dimensional BF model, although it requires more computational effort. We present several results from modelling a stented artery using ISR3D in figure 1, which shows the artery both before and after restenosis has occurred.

From a multiscale modelling perspective, ISR3D combines four submodels, each operating on a different time scale: SMC proliferation, which models the cell cycle, cell growth and physical forces between cells; initial thrombus formation (ITF) due to the backflow of blood; drug diffusion (DD) of the drug-eluting stent through the tissue and applied to the smooth muscle cells; and BF and the resulting wall shear stress on SMCs. We show the time scales of each submodel and the relations between them in figure 2. The SMC submodel uses an agent-based algorithm on the cellular scale, which undergoes validation on the tissue level. All other submodels act on a Cartesian grid representation of those cells. For the BF submodel, we use 1 237 040 lattice sites, and for the SMC submodel, we use 196 948 cells. The exchanges between the submodels are in the order of 10–20 MB. The SMC sends a list of cell locations and sizes (stored as 8-byte integers) to the ITF, which sends the geometry (stored as a three-dimensional matrix of 8-byte integers) to BF and DD. In turn, BF and DD, respectively, send a list of wall shear stress and drug concentrations (stored as 8-byte doubles) to SMC. Each coupling communication between SMC and the other submodels takes place once per SMC iteration.

The submodels act independently, apart from exchanging messages, and are heterogeneous. The SMC code is implemented in C++, the DD code in Java and the ITF code in Fortran. The BF code, which unlike the other codes runs in parallel, uses the Palabos lattice-Boltzmann application (<http://www.palabos.org/>), written in C++. The MML specification of ISR3D contains a few conversion modules not mentioned earlier, which perform basic data transformations necessary to ensure that the various single-scale models do

not need to be aware of other submodels and their internal representation or scales. Specifically, the submodels operate within the same domain, requiring the application to keep the grid and cell representation consistent, as well as their dimensions.

5.1. Tests

We have performed a number of tests to measure both the runtime and the efficiency of our multiscale ISR3D simulation. The runs that were performed here were short versions of the actual simulations, with a limited number of iterations. The runs contributed to the integration testing of the code and allowed us to estimate the requirements for future computing resource proposals.

We have run our tests in five different scenarios, using the EGI resource in Krakow (Zeus, one scenario), a Dutch PRACE tier-1 machine in Amsterdam (Huygens, two scenarios) or a combination of both (two scenarios). We provide the technical specifications of the resources in table 1. Since the runtime behaviour of ISR3D is cyclic, determined by the number of SMC iterations, we measured the runtime of a single cycle for each scenario. Because only the BF model is parallelized, the resources we use are partially idle whenever we are not executing the BF model. To reduce this overhead of ‘idle time’, we created two *double mapping* scenarios, each of which runs two simulations in alternating fashion using the same resource reservation. In these cases, the BF calculations of one simulation takes place while the other simulation executes one or more of the other submodels. We use a wait/notify signalling system within MUSCLE to enforce that only one of the two simulations indeed executes its parallel BF model. We have run one double mapping scenario locally on Huygens, and one distributed over Huygens and Zeus.

5.1.1. Results

We present our performance measurements for the five scenarios in table 3. The runtime of our simulation is reduced by almost 50 per cent when we use the Huygens machine instead of Zeus. This is because we run the BF code on Huygens using 32 cores, and on Zeus using 4 cores. However, the usage of the reservation was considerably lower

Table 1. Computational characteristics of the machines we use in our multiscale simulations for ISR3D and HemeLB. Clock frequency is given in the second column, the number of cores used in the third column and the amount of memory per node in the fourth column. The administrative details are listed in table 2.

name	processor	freq. (GHz)	cores	mem/node (GB)	middleware
HECTOR	AMD Interlagos	2.3	512/2048	32	UNICORE
Huygens	IBM Power6	4.7	32	128	UNICORE
Henry	Intel Xeon	2.4	1	6	none
Zeus	Intel Xeon	2.4	4	16	QCG-Comp.

Table 2. Administrative information for the resources described in table 1.

name	provider	location	infrastructure
HECTOR	EPCC	Edinburgh, UK	PRACE Tier-1
Huygens	SARA	Amsterdam, The Netherlands	PRACE Tier-1
Henry	UCL	London, UK	Local workstation
Zeus	Cyfronet	Krakow, Poland	EGI (PL-Grid)

on Huygens than on Zeus for two reasons: first, the allocation on Huygens was larger, leaving more cores idle when the sequential submodels were computed; second, the ITF solver uses the gfortran compiler, which is not well optimized for Huygens architecture. As a result, it requires only 4 min on Zeus and 12 min on Huygens. The performance of the other sequential submodels is less platform dependent. When we run our simulation distributed over both resources, we achieve the lowest runtime. This is because we combine the fast execution of the BF module on Huygens with the fast execution of the ITF solver on Zeus.

When we use double mapping, the runtime per simulation increases by about 6 per cent (using only Huygens) to 18 per cent (using both resources). However, the double-mapping improves the usage of the reservation by a factor of approximately 1.7. Double-mapping is therefore an effective method to improve the resource usage without incurring major increases to the time to completion of each simulation. The coupling overhead is relatively low throughout our runs, consisting of no more than 11 per cent of the runtime throughout our measurements. Using our approach, we are now modelling different ISR scenarios, exploring a range of modelling parameters.

5.2. Clinical directions

We primarily seek to understand which biological pathways dominate in the process leading to ISR. If successful, this will have two effects on clinical practice: first, it suggests which factors are important for ISR, in turn giving clinicians more accurate estimates of what the progression of the disease can be; second, it may spur further directed clinical research of certain pathways, which will help the next iteration of the model give more accurate results.

The methods for achieving this divide naturally in two directions: general model validation and experiments; and

virtual patient cohort studies. For general model validation, we consult the literature and use basic experimental data, such as measurements from animal studies. In addition, we intend to use virtual patient cohort studies to assess the ISR-risk factors of virtual patients with different characteristics. In clinical practice, this will not lead to personalized estimates, but rather to patient classifiers on how ISR3D will progress. Once the primary factors leading to ISR have been assessed, a simplified model could be made based on ISR3D, which takes less computational effort and runs within a hospital.

6. Modelling of cerebrovascular blood flow

Our second hemodynamic example aims to incorporate not only the local arterial structure in our models, but also properties of the circulation in the rest of the human body. The key feature of this application is the multiscale modelling of BF, delivering accuracy in the regions of direct scientific or clinical interest while incorporating global BF properties using more approximate methods. Here we provide an overview of our multiscale model and report on its performance. A considerable amount of previous work has been done where groups combined bloodflow solvers of different types, for example, in the area of cardiovascular [34–36] or cerebrovascular bloodflow [12,37].

We have constructed a distributed multiscale model in which we combine the open source HemeLB lattice-Boltzmann application for BF modelling in three-dimensions [38,39] with the open source one-dimensional Python Navier–Stokes (pyNS) BF solver [40]. HemeLB is optimized for sparse geometries, such as vascular networks and has been shown to scale linearly up to at least 32 768 cores [41]. PyNS is a discontinuous Galerkin solver which is geared towards modelling large arterial structures. It uses aortic BF input based on a set of patient-specific parameters, and it combines one-dimensional wave propagation elements to model arterial vasculature with zero-dimensional resistance elements to model veins. The numerical code supports thread-level parallelization and is written in Python in conjunction with the numpy numerical library.

6.1. Simulations

We have run a number of coupled simulations using both HemeLB and pyNS as submodels. Within pyNS, we use a customized version of the ‘Willis’ model, based on [42], with a mean pressure 90 mmHg, a heart rate of 70 beats per minute and a cardiac output of 5.68 l min^{-1} . Our model includes the major arteries in the human torso, head and both arms, as well as a full model for the circle of Willis,

Table 3. Runtimes with different scenarios. The name of the scenario is given in the first column, the time spent on BF in the second, and the total time spent on the other submodels in the third column (both rounded to the nearest minute). We provide the coupling overhead in the fourth column and the total simulation time per cycle in the fifth column. In the sixth column, we provide the average fraction of reserved resources doing computations (not idling) throughout the period of execution. All time are given in seconds.

scenario	BF	other	coupling	total	usage (%)
Zeus	2100	1140	79	3240	80
Huygens	480	1260	73	1813	27
Huygens-double	480	1320	131	1931	45
Zeus–Huygens	480	960	92	1532	32
Zeus–Huygens-double	480	1080	244	1804	56

Table 4. Performance measurements of coupled simulations which consist of HemeLB running on HECToR and pyNS running on a local UCL workstation. The type of simulation, single-scale (ss) or coupled multiscale (ms) is given in the first columns. The number of cores used by HemeLB and the initialization time are, respectively, given in the second and third column. The time spent on HemeLB and coupling work are given, respectively, in the fourth and fifth column, the total time in the sixth column and the efficiency in the seventh column. The times for HemeLB model execution in the multiscale runs are estimates, which we derived directly from the single-scale performance results of the same problem on the same resources.

ss/ms	cores	init (time spent)	HemeLB* (time spent)	coupling (time spent)	total (time spent)	coupling efficiency
ss	512	47.9	2223	n.a.	2271	n.a.
ms	512	51.2	2223	24	2298	98.8%
ss	2048	46.4	815	n.a.	862	n.a.
ms	2048	50.5	815	37	907	95.0%

which is a major network of arteries in the human head. For pyNS, we use a time step size of 2.3766×10^{-4} s.

We have modified a section of the right mid-cerebral artery in pyNS to allow it to be coupled to HemeLB in four places, exchanging pressure values in these boundary regions. In HemeLB we simulate a small network of arteries, with a voxel size of 3.5×10^{-5} m and consisting of about 4.2 million lattice sites which occupy 2.3 per cent of the simulation box volume. The HemeLB simulation runs with a time step of 2.3766×10^{-6} s, a Mach number of 0.1 and a relaxation parameter τ of 0.52. We run pyNS using a local machine at UCL (Henry), while we run HemeLB for 400 000 time steps on the HECToR supercomputer in Edinburgh. The round-trip time for a network message between these two resources is on average 11 ms. We provide technical details of both machines in table 2. Both codes exchange pressure data at an interval of 100 HemeLB time steps (or 1 pyNS time step). Because HemeLB time steps can take as little as 0.0002 s, we adopted MPWide to connect our submodels, which run concurrently, and minimize the communication response time. The exchanged data are represented using 8-byte doubles and has a small aggregate size (less than 1 kb). As a comparison, we have also run HemeLB as a stand-alone single-scale simulation (labelled 'ss'), retrieving its boundary values from a local configuration file. The pyNS code requires 116 s to simulate 4000 time steps of our modified circle of Willis problem when run as a stand-alone code.

We present our results in table 4. For 512 cores, the single-scale HemeLB simulation takes 2271 s to perform its 400 000 lattice-Boltzmann time steps. The coupled HemeLB-pyNS simulation is only marginally slower, reaching completion

in 2298 s. We measure a coupling overhead of only 24 s, which is the time to do 4002 pressure exchanges between HemeLB and pyNS. This amounts to about 6 ms per exchange, well below even the round-trip time of the network between UCL and EPCC alone. The communication time on the HemeLB side is so low because pyNS runs faster per coupling iteration than HemeLB, and the incoming pressure values are already waiting at the network interface when HemeLB begins to send out its own. As a result, the coupling overhead is only 24 s, and the multiscale simulation is only 1.2 per cent slower than a single-scale simulation of the same network domain.

When using 2048 cores, the runtime for the single-scale HemeLB simulation is 815 s, which is a speed up of 2.63 compared with the 512 core run. The coupling overhead of the multiscale simulation is relatively higher than that of the 512 core run due to a larger number of processes with which pressures must be exchanged. This results in an overall coupling efficiency of 0.95, which is lower than for the 512 core run. However, the 2048 core run contains approximately 2000 sites per core, which is a regime where we no longer achieve linear scalability [41] to begin with. As a future task, we plan to coalesce these pressure exchanges with the other communications in HemeLB, using the coalesced communication pattern [43].

6.2. Clinical directions

We aim to understand the flow dynamics in cerebrovascular networks and to predict the flow dynamics in brain aneurysms for individual patients. The ability to predict the flow dynamics

in cerebrovascular networks is of practical use to clinicians, as it allows them to more accurately determine whether surgery is required for a specific patient suffering from an aneurysm. In addition, our work supports a range of other scenarios, which in turn may drive clinical investigations of other vascular diseases.

Our current efforts focus on enhancing the model by introducing velocity exchange and testing our models for accuracy. As a first accuracy test, we compared different boundary conditions and flow models within HemeLB [39]. Additionally we used our HemeLB-pyNS setup to compare different blood rheology models, which we describe in detail in [44]. Next steps include more patient-specific studies, where we wish to compare the flow behaviour within patient-specific networks of arteries in our multi-scale simulations with the measured from those same patients. We have already established several key functionalities to allow patient-specific modelling. For example, HemeLB is able to convert three-dimensional rotational angiographic data into initial conditions for the simulation, while pyNS provides support for patient-specific global parameters and customized arterial tree definitions.

References

1. Sloot PMA, Hoekstra AG. 2010 Multi-scale modelling in computational biomedicine. *Brief. Bioinform.* **11**, 142–152. (doi:10.1093/bib/bbp038)
2. Kohl P, Noble D. 2009 Systems biology and the virtual physiological human. *Mol. Syst. Biol.* **5**, 292. (doi:10.1038/msb.2009.51)
3. Tahir H, Hoekstra AG, Lorenz E, Lawford PV, Hose DR, Gunn J, Evans DJW. 2011 Multi-scale simulations of the dynamics of in-stent restenosis: impact of stent deployment and design. *Interface Focus* **1**, 365–373. (doi:10.1098/rsfs.2010.0024)
4. Migliavacca F, Dubini G. 2005 Computational modeling of vascular anastomoses. *Biomech. Model. Mechanobiol.* **3**, 235–250. (doi:10.1007/s10237-005-0070-2)
5. Obiol-Pardo C, Gomis-Tena J, Sanz F, Saiz J, Pastor M. 2011 A multiscale simulation system for the prediction of drug-induced cardiotoxicity. *J. Chem. Inform. Model.* **51**, 483–492. (doi:10.1021/ci100423z)
6. Noble D. 2002 Modeling the heart—from genes to cells to the whole organ. *Science* **295**, 1678–1682. (doi:10.1126/science.1069881)
7. Finkelstein A, Hetherington J, Li L, Margoninski O, Saffrey P, Seymour R, Warner A. 2004 Computational challenges of systems biology. *Computer* **37**, 26–33. (doi:10.1109/MC.2004.1297236)
8. Hetherington J *et al.* 2007 Addressing the challenges of multiscale model management in systems biology. *Comp. Chem. Eng.* **31**, 962–979. (doi:10.1016/j.compchemeng.2006.10.004)
9. Southern J, Pitt-Francis J, Whiteley J, Stokely D, Kobashi H, Nobes R, Kadooka Y, Gavaghan D. 2008 Multi-scale computational modelling in biology and physiology. *Progr. Biophys. Mol. Biol.* **96**, 60–89. (doi:10.1016/j.pbiomolbio.2007.07.019)
10. Hegewald J, Krafczyk M, Tölke J, Hoekstra A, Chopard B. 2008 An agent-based coupling platform for complex automata. In *Proc. 8th Int. Conf. on Computational Science, Part II, ICCS '08, Kraków, Poland, June 23–25, 2008*, pp. 227–233. Berlin, Germany: Springer.
11. Borgdorff J *et al.* 2012 A distributed multiscale computation of a tightly coupled model using the multiscale modeling language. *Proc. Comp. Sci.* **9**, 596–605. (doi:10.1016/j.procs.2012.04.064)
12. Grinberg L, Morozov V, Fedosov D, Inley JA, Papka ME, Kumaran K, Karniadakis GE. 2011 A new computational paradigm in multiscale simulations: application to brain blood flow. In *2011 Int. Conf. for High Performance Computing, Networking, Storage and Analysis (SC), Seattle, WA, November 12–18, 2011*, pp. 1–12. Washington, DC: IEEE Computer Society.
13. Ciepela E, Hareźlak D, Kocot J, Bartyński T, Kasztelnik M, Nowakowski P, Gubala T, Malawski M, Bubak M. 2010 Exploratory programming in the virtual laboratory. In *Proc. 2010 Int. Multiconf. on Computer Science and Information Technology (IMCSIT), Wisła, Poland, October 18–20, 2010*, pp. 621–628. Washington, DC: IEEE Computer Society.
14. Groen D, Zasada SJ, Coveney PV. 2012 Survey of multiscale and multiphysics applications and communities. See <http://arxiv.org/abs/1208.6444>.
15. Hucka M *et al.* 2003 The systems biology markup language (SBML): a medium for representation and exchange of biochemical network models. *Bioinformatics* **19**, 524–531. (doi:10.1093/bioinformatics/btg015)
16. Lloyd CM, Halstead MDB, Nielsen PF. 2004 CellML: its future, present and past. *Progr. Biophys. Mol. Biol.* **85**, 433–450. (doi:10.1016/j.pbiomolbio.2004.01.004)
17. Hoekstra AG, Lorenz E, Falcone J-L, Chopard B. 2007 Toward a complex automata formalism for multiscale modeling. *Int. J. Multiscale Comp. Eng.* **5**, 491–502. (doi:10.1615/IntJMultCompEng.v5.i6.60)
18. Hoekstra AG, Caiazzo A, Lorenz E, Falcone J-L, Chopard B. 2010 *Complex automata: multi-scale modeling with coupled cellular automata* (Understanding complex systems), pp. 29–57. Berlin, Germany: Springer.
19. Evans DJW *et al.* 2008 The application of multiscale modelling to the process of development and prevention of stenosis in a stented coronary artery. *Phil. Trans. R. Soc. A* **366**, 3343–3360. (doi:10.1098/rsta.2008.0081)
20. Caiazzo A *et al.* 2011 A complex automata approach for in-stent restenosis: two-dimensional multiscale modeling and simulations. *J. Comp. Sci.* **2**, 9–17. (doi:10.1016/j.jocs.2010.09.002)
21. Borgdorff J, Falcone J-L, Lorenz E, Chopard B, Hoekstra AG. 2011 A principled approach to distributed multiscale computing, from formalization to execution. In *Proc. IEEE 7th Int. Conf. on e-Science Workshops, Stockholm, Sweden, 5–8 December, 2011*, pp. 97–104. Stockholm, Sweden: IEEE Computer Society Press.
22. Falcone J-L, Chopard B, Hoekstra A. 2010 Mml: towards a multiscale modeling language. *Proc. Comp. Sci.* **1**, 819–826. (doi:10.1016/j.procs.2010.04.089)
23. Zasada SJ, Mamonski M, Groen D, Borgdorff J, Saverchenko I, Piontek T, Kurowski K, Coveney PV.

- 2012 Distributed infrastructure for multiscale computing. In *Proc. 2012 IEEE/ACM 16th Int. Symp on Distributed Simulation and Real Time Applications, DS-RT '12, Dublin, Ireland, October 25–27, 2012*, pp. 65–74. Washington, DC: IEEE Computer Society.
24. Groen D, Rieder S, Grosso P, de Laat C, Portegies Zwart P. 2010 A light-weight communication library for distributed computing. *Comp. Sci. Disc.* **3**. (doi:10.1088/1749-4699/3/1/015002)
 25. Groen D, Portegies Zwart S, Ishiyama T, Makino J. 2011 High performance gravitational N-body simulations on a planet-wide distributed supercomputer. *Comp. Sci. Disc.* **4**, 015001. (doi:10.1088/1749-4699/4/1/015001)
 26. Kurowski K, Piontek T, Kopta P, Mamonski M, Bosak B. 2010 Parallel large scale simulations in the PL-grid environment. *Computational Methods Sci Technol*, Special Issue 2010, pp. 47–56.
 27. Zasada SJ, Coveney PV. 2009 Virtualizing access to scientific applications with the application hosting environment. *Comp. Phys. Commun.* **180**, 2513–2525. (doi:10.1016/j.cpc.2009.06.008)
 28. Suter J, Groen D, Kabalan L, Coveney PV. 2012 Distributed multiscale simulations of clay-polymer nanocomposites. In *Materials Research Society Spring Meeting, vol. 1470, San Francisco, CA, April 9–13, 2012* (MRS Online Proceedings Library). Cambridge, UK: Cambridge University Press.
 29. Ben Belgacem M, Chopard B, Parmigiani A. 2012 Coupling method for building a network of irrigation canals on a distributed computing environment. In *Cellular automata* (eds G Sirakoulis, S Bandini). Lecture Notes in Computer Science, vol. 7495, pp. 309–318. Berlin, Germany: Springer.
 30. WHO, World Heart Federation; World Stroke Organization (ed.) 2012 *Global atlas on cardiovascular disease prevention and control. Policies, strategies and interventions*. Geneva, Switzerland: World Health Organization.
 31. Moustapha A *et al.* 2001 Percutaneous and surgical interventions for in-stent restenosis: long-term outcomes and effect of diabetes mellitus. *J. Am. College Cardiol.* **37**, 1877–1882. (doi:10.1016/S0735-1097(01)01231-1)
 32. Kastrati A, Hall D, Schömig A. 2000 Long-term outcome after coronary stenting. *Curr. Control. Trials Cardiovasc. Med.* **1**, 48–54. (doi:10.1186/CVM-1-1-048)
 33. Jukema JW, Verschuren JJW, Ahmed TAN, Quax PHA. 2011 Restenosis after PCI. Part 1: pathophysiology and risk factors. *Nat. Rev. Cardiol.* **9**, 53–62. (doi:10.1038/nrcardio.2011.132)
 34. Shi Y, Lawford P, Hose R. 2011 Review of zero-d and 1-d models of blood flow in the cardiovascular system. *Biomed. Eng. Online* **10**, 33. (doi:10.1186/1475-925X-10-33)
 35. van de Vosse FN, Stergiopoulos N. 2011 Pulse wave propagation in the arterial tree. *Annu. Rev. Fluid Mech.* **43**, 467–499. (doi:10.1146/annurev-fluid-122109-160730)
 36. Sugimoto K, Liang F, Takahara Y, Yamazaki K, Senzaki H, Takagi S, Liu H. In press. Assessment of cardiovascular function by combining clinical data with a computational model of the cardiovascular system. *J. Thorac. Cardiovasc. Surg.*
 37. Alastruey J, Moore SM, Parker KH, David T, Peiró J, Sherwin SJ. 2008 Reduced modelling of blood flow in the cerebral circulation: coupling 1-d, 0-d and cerebral auto-regulation models. *Int. J. Numer. Methods Fluids* **56**, 1061–1067. (doi:10.1002/fld.1606)
 38. Mazzeo MD, Coveney PV. 2008 HemeLB: a high performance parallel lattice-Boltzmann code for large scale fluid flow in complex geometries. *Comp. Phys. Commun.* **178**, 894–914. (doi:10.1016/j.cpc.2008.02.013)
 39. Carver HB, Nash RW, Bernabeu MO, Hetherington J, Groen D, Krüger T, Coveney PV. Submitted. Choice of boundary condition and collision operator for lattice-Boltzmann simulation of moderate Reynolds number flow in complex domains. *Phys. Rev. E*. (<http://arxiv.org/abs/1211.0205>)
 40. Botti L, Piccinelli M, Ene-Iordache B, Remuzzi A, Antiga L. 2010 An adaptive mesh refinement solver for large-scale simulation of biological flows. *Int. J. Numer. Methods Biomed. Eng.* **26**, 86–100. (doi:10.1002/cnm.1257)
 41. Groen D, Hetherington J, Carver HB, Nash RW, Bernabeu MO, Coveney PV. 2012 Analyzing and modeling the performance of the HemeLB lattice-Boltzmann simulation environment. See <http://arxiv.org/abs/1209.3972>.
 42. Mulder G, Bogaerds ACB, Rongen P, van de Vosse FN. 2011 The influence of contrast agent injection on physiological flow in the circle of willis. *Med. Eng. Phys.* **33**, 195–203. (doi:10.1016/j.medengphy.2010.09.021)
 43. Carver HB, Groen D, Hetherington J, Nash RW, Bernabeu MO, Coveney PV. 2012 Coalesced communication: a design pattern for complex parallel scientific software. See <http://arxiv.org/abs/1210.4400>.
 44. Bernabeu MO, Nash RW, Groen D, Carver HB, Hetherington J, Krüger T, Coveney PV. 2013 Impact of blood rheology on wall shear stress in a model of the middle cerebral artery. *Interface Focus* **3**, 20120094. (doi:10.1098/rsfs.2012.0094)